INTERPRETATION OF ELECTRIC FIELD GRADIENTS AT DEUTERIUM AS MEASURED BY SOLID-STATE NMR SPECTROSCOPY

Leslie G. Butler[a]; Ellen A. Keiter[b]

[a] Department of Chemistry, Louisiana State University, Baton Rouge, Louisiana [b] Department of Chemistry, Eastern Illinois University, Charleston, Illinois

PLEASE SCROLL DOWN FOR ARTICLE

INTERPRETATION OF ELECTRIC FIELD GRADIENTS AT DEUTERIUM AS MEASURED BY SOLID-STATE NMR SPECTROSCOPY

LESLIE G. BUTLER*

Department of Chemistry, Louisiana State University, Baton Rouge, Louisiana 70803-1804

and ELLEN A. KEITER*

Department of Chemistry, Eastern Illinois University, Charleston, Illinois 61920

A simple interpretative scheme is presented to describe the deuterium quadrupole coupling constant and asymmetry parameter in a wide variety of chemical environments.

KEYWORDS: solid-state deuterium NMR, quadrupole coupling constant, electric field gradient

INTRODUCTION

The objective of this tutorial is to make the connection between molecular structure at a deuterated site and two solid-state deuterium NMR spectroscopic parameters: the quadrupole coupling constant and the asymmetry parameter. Deuterium NMR spectroscopy as a probe of solid-state structures and dynamics has a number of advantages: (1) Solid-state deuterium NMR line shapes and spin-lattice relaxation times are sensitive to dynamical processes over a very wide range of exchange rates, more than ten orders of magnitude, making solid-state deuterium NMR very popular for motional studies in polymers, biomaterials, and other solids. (2) Molecular orbital calculations make possible comparison between experimental and theoretical deuterium electric field gradients. (3) Methods for acquiring spectra have improved dramatically in recent years; commercial solid-state NMR spectrometers can acquire high quality data from powders.

The jargon of deuterium NMR and NQR spectroscopy includes the terms electric field gradient tensors, nuclear electric quadrupole moments, quadrupole coupling constants, and asymmetry parameters. If we first examine a collection of experimental values for the quadrupole coupling constant for deuterium bound to another atom, for example, atoms of the first and second row (see Table 1), we note a regular pattern as shown in Figure 1. This pattern implies a simple origin and the potential for exploiting deuterium NMR spectroscopy in a variety of ways. As a starting

---

* Author for correspondence.

Table 1 Representative values for the deuterium quadrupole coupling constant in X–D bonds

X	C_Q/kHz	Example	Reference
H	225	HD (g)[a]	11
Li	33	LiD (g)	31
Be	71	BeD (theory)	52
B	105 ± 1	$D_3B \cdot N(CH_3)_3$(s)	53
C	173 ± 1	(9,9-D_2)fluorene (s)	17
N	282 ± 12	NH_2D (g)	54
O	318.6 ± 2.6	HDO (g)	25
F	354.24 ± 8	DF (g)	55
Al	72	$LiAlD_4$(s)	56
Si	91 ± 2	$C_6H_5SiD_3$ (lc)	57
P	115 ± 2	$C_6H_5PD_2$ (lc)	57
S	146 ± 3	C_6H_5SD (lc)	57
Cl	190	DCl (s)	58
Br	153	DBr (s)	58
I	113	DI (s)	58

[a]g = gas, s = solid, lc = liquid crystal.
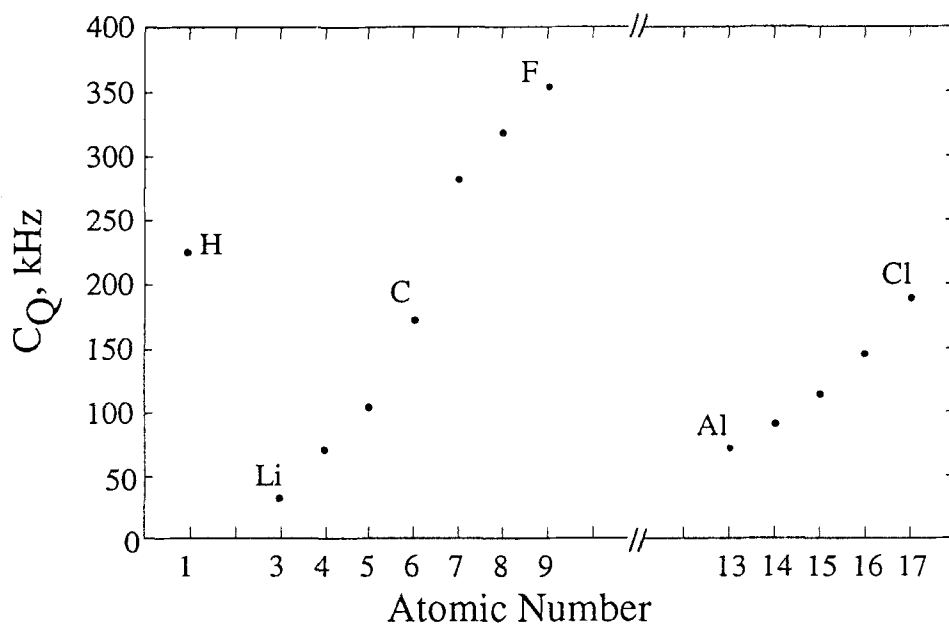
Figure 1 Deuterium quadrupole coupling constants for typical bonds as a function of atomic number. All data shown are for terminal X–D bonds for the species listed in Table I. Bridging sites, such as hydrogen bonds, are not shown here because of the potential for greatly different values of C_Q.

point, consider Figure 2, which shows a representative D–X bond, and these statements:

- The quadrupole coupling constant depends upon the nuclear charge of atom X.
- The nuclear charge is partly shielded by core and valence electrons on X.
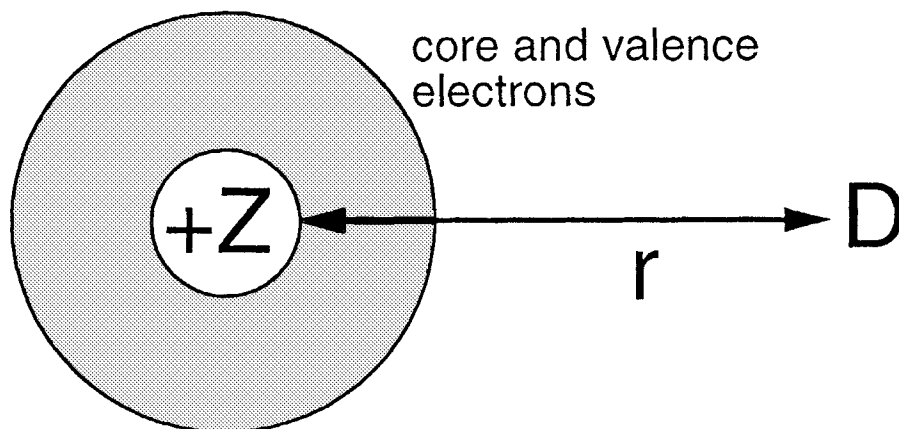
Figure 2 A simple interpretative scheme for the deuterium quadrupole coupling constant based on a large, positive contribution from the nuclear charge and a slightly smaller, negative contribution from the core and valence electrons. Both terms are reduced in magnitude by increasing the bond length.

- The shorter the X–D bond length, the larger the deuterium quadrupole coupling constant.
- The electronic population of the 1s orbital located on D has no effect on the deuterium quadrupole coupling constant because of the spherical symmetry of this orbital.

Each of these statements can be traced to simple electrostatic interactions, as will be discussed herein.

One of the first extensive discussions of deuterium quadrupole coupling constants was given by Bersohn in 1958.[1] In the present work, the interpretation of Bersohn is augmented by additional experimental data collected over the intervening years.

Definition of Electric Field Gradients and Electric Quadrupole Moments

A progression of electrostatic interactions
For the purpose of understanding the properties of electric field gradients and electric quadrupole moments, it is helpful to place these terms in a linear progression used to describe any arbitrary electric charge distribution. Let us start with the electric quadrupole moment and its place in a progression used to model the charge distribution, $\rho(r)$, of a nucleus:

$$\rho(r) = Z + \mu r + Qr^2 + \ldots \tag{1}$$

For atomic nuclei, one is already familiar with the concept of a nuclear charge, Z, while the notion of an atomic electric dipole moment, μ, is less so. Of course, molecular electric dipole moments are often encountered in spectroscopy and molecular modeling; important for this discussion is the fact that the electrostatics are the same for both atomic and molecular dipole moments. That brings us to the nuclear quadrupole moment, Q, which can be non-zero if the nuclear spin angular

momentum, I, is greater than one-half. Similarly, electric charges surrounding the nucleus create electric fields that can be described by the following progression: electric potential, electric field, electric field gradient, and higher order terms. The electric potential and field are mathematically described by a scalar and a vector, respectively; the electric field gradient is expressed as a tensor.

NMR and other spectroscopic observables are related to the energy of various interactions. We are familiar with the energy of the interaction between an electric dipole moment and an electric field shown schematically in Figure 3b. Also shown is the interaction of an electric charge in an electric potential, Figure 3a. Finally, a two-dimensional representation of a quadrupolar interaction is shown in the lowest energy configuration, Figure 3c. Higher energy configurations can be obtained by rotating the electric quadrupole moment about an axis normal to the plane of the paper. NMR/NQR of quadrupolar nuclei is based on the quantized energy levels corresponding to different orientations of the nuclear electric quadrupole moment with respect to the electric field gradient.

There are some specific aspects of the electrostatic interactions that are pertinent for nuclei in atoms and molecules. First, a nucleus, even though surrounded by many electric charges, is always situated in space such that the electric potential at the nucleus is zero. If the electric potential happens to be non-zero, the nucleus experiences a force that pushes it to a region of zero electric potential. Second, the nuclear electric dipole moment is required to be zero based upon the symmetry of the nuclear wavefunction; a non-zero dipole moment violates time-reversal symmetry arguments. Third, the trace of the electric field gradient tensor at a nucleus is zero; additional details about the trace will be given below. Fourth, accurate values of Q are known for some nuclei but not others; a variety of measurement techniques are employed depending upon nuclear spin and atomic electron configuration. Pyykkö has recently summarized values of Q for the first twenty elements.[2] For deuterium, $Q = 2.86 \times 10^{-31}$ m[2].[3,4]

The electric field gradient tensor
A tensor is a 3×3 matrix that is useful for describing an interaction that has a directional dependence.[5] For deuterium in a C–D bond, we find that the electric field gradient along the C–D bond is larger than for a direction perpendicular to the C–D bond.[6,7] Tensor orientations are expressed relative to an axis system and there are several axis systems of note. The molecular axis system is preferred for analyzing the results of molecular orbital calculations while the laboratory axis system has its place in the NMR experiment for defining the orientation of static and RF magnetic fields. However, we will start with yet another axis system called the principal axis system. One feature of the principal axis system is that the 3×3 matrix is diagonal; all off-diagonal elements are zero. The electric field gradient tensor in the principal axis system is

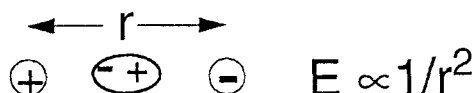$$V^{PA} = \begin{bmatrix} q_{xx} & 0 & 0 \\ 0 & q_{yy} & 0 \\ 0 & 0 & q_{zz} \end{bmatrix} \qquad (2)$$

where q is an electric field gradient component. A second feature of the principal axis system is a convention for ordering the diagonal elements of the electric field gradient tensor. By convention, the largest element (magnitude) is defined as the

a) Charge in an electric potential:
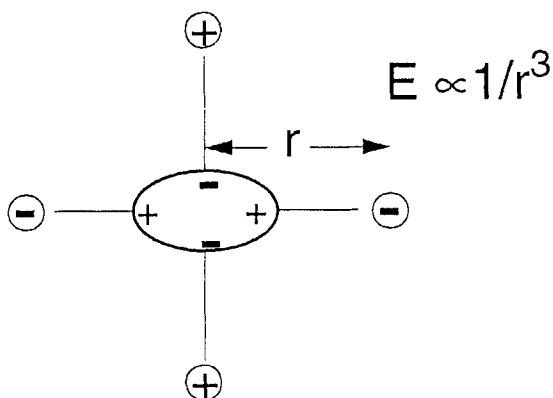
$$E \propto 1/r$$

b) Dipole moment in an electric field:

$$E \propto 1/r^2$$

c) Quadrupole moment in an electric field gradient:

$$E \propto 1/r^3$$

Figure 3 Electrostatic interactions in a progression leading up to the quadrupolar interaction. Two-dimensional representations of three interactions are shown with an emphasis on the distance dependence of the interaction energy. The electric quadrupole moment is shown here as a prolate charge distribution (football shaped object) interacting with an electric field gradient created by the four isolated charges. Like the dipolar interaction, the quadrupolar interaction is shown in the lowest energy geometry; higher energy configurations can be obtained by rotating the electric quadrupole moment about an axis normal to the plane of the paper or about an axis aligned with the vertical.

component along the z axis of the principal axis system and the second largest element as the component along the y axis; thus

$$|q_{zz}| \geq |q_{yy}| \geq |q_{xx}| \tag{3}$$

We noted above that the trace of the electric field gradient tensor is zero, therefore

the following relationship holds:

$$q_{xx} = q_{yy} = q_{zz} = 0 \tag{4}$$

Since the trace is zero, only two parameters are needed to describe the electric field gradient tensor in the principal axis system. Based on the NMR Hamiltonians, 'size' and 'shape' are expressed by the quadrupole coupling constant, $C_Q = e^2 q_{zz} Q/h$, and the asymmetry parameter, η,

$$\eta = \frac{q_{xx} - q_{yy}}{q_{zz}} \tag{5}$$

For the convention given in eq 3, the value of the asymmetry parameter ranges from 0 to 1. For $\eta = 0$, the two minor elements q_{xx} and q_{yy} are equal and have a value of $\frac{-1}{2} q_{zz}$. Most NMR and NQR experiments yield values for the quadrupole coupling constant and the asymmetry parameter. A few experiments, single crystal NMR amd microwave spectroscopy, also yield the orientation of the electric field gradient tensor with respect to the molecular axis system.

At this point, we can use symmetry arguments to predict values, zero or non-zero, for the quadrupole coupling constant, C_Q, and the asymmetry parameter, η. First, consider a deuterium nucleus surrounded by six electric charges in an octahedral array, as shown in Figure 4a. In this high symmetry example, we expect $q_{xx} = q_{yy} = q_{zz}$. If this is so, and since eq 4 requires the sum of the three elements to be zero, then it follows that all elements must be equal to zero. Hence, $C_Q = 0$ and $\eta = 0$ for the deuteron in Figure 4a. Likewise, a deuteron at a site with T_d symmetry will have zero values for C_Q and η. (One may wish to consult a text on group theory and note the similarity between T_d and O_h point groups insofar as the x, y, and z axes are transformed.[8] Interestingly, C_Q and η are zero for the gas-phase species, D^+, $D^\bullet$, and D^-; the quadrupolar interaction does not directly depend upon charge at deuterium when the charge resides in the deuterium-centered, spherically-symmetric s orbital.

For metal hydride complexes, symmetry arguments also require that η is zero in M–D and linear M–D–M systems (Figure 4b). In these cases, the axial symmetry requires that the two elements perpendicular to the M–D–M axis be equal. If the third element has a different value, and it usually does, then it must be labelled as q_{zz} to satisfy eqs 3 and 4. If fact, η will be zero if there is C_3 or higher symmetry at the deuteron. For non-linear M–D–M bonds (Figure 4c), the values of C_Q and η can be non-zero.

Electric field gradients from molecular orbital calculations
From one viewpoint, the purpose of a molecular orbital calculation of an electronic ground state is to determine the electric charge density distribution and from the distribution, many other properties are calculated. The output of a molecular orbital calculation, wavefunction and nuclear positions, can be used to calculate the elements of the electric field gradient tensor.[6,7,9,10] Each element is the sum of nuclear and electronic terms; the latter is expressed as an expectation value of the wavefunction:

$$q_{zz} = + \sum_n Z_n \frac{3z_n^2 - r_n^2}{r_n^5} - e\left[\Psi^* \left| \sum_i \frac{3z_i^2 - r_i^2}{r_i^5} \right| \Psi \right] \tag{6}$$
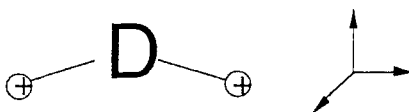
a) octahedral symmetry: $C_Q = 0$ kHz, $\eta = 0$
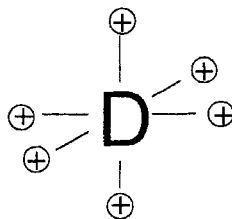
b) axial symmetry: $C_Q \neq 0$ kHz, $\eta = 0$

c) low symmetry: $C_Q \neq 0$ kHz, $\eta \neq 0$

Figure 4   Special electric field gradient tensors for some deuterium sites. The values for C_Q and η are obtained by symmetry arguments, the convention for labelling the elements of the electric field gradient tensor, and the requirement that the trace of the tensor is zero.

shown here in atomic units for the q_{zz} element where e is the electronic charge ($e = +1$ au), n is the index over the other nuclei, the nuclear charge is given by Z_n, and i is the index over the electrons of the molecule. The origin is defined as the deuteron site; r_n and r_i are vectors to neighboring nuclei and electrons. The key features of eq 6 follow from the two-dimensional representation shown in Figure 3c. The magnitude of the electric field gradient tensor element q_{zz} depends upon the charge, both nuclear and electronic, that lies along the z axis minus two components from the perpendicular axes. The compensation from charges along perpendicular axes comes from the $3z^2 - r^2$ terms in the numerators of the nuclear and electronic components. The equation for the electric field gradient tensor element q_{xx} is similar to that given in eq 6, but with the term $3x^2 - r^2$ in the numerator; an off-diagonal element such as q_{xy} has the term xy in the numerator. For all elements of the electric

field gradient tensor, the overall distance dependence is a steep r^{-3}, hence the quadrupolar interaction operates over a relatively short range.

Trends in C_Q and η in X–D Bonds

In Figure 2, we introduced three initial concepts for following the pattern shown in Figure 1. We stated that C_Q depends upon nuclear charge, shielding of the nuclear charge by core and valence electrons, and the X–D bond length. We also implied by omission that the other parameter, η, was not important and is, in fact, near zero for the species shown in Figure 1.

For the purpose of assessing the importance of nuclear charge, we can calculate the nuclear contribution to the electric field gradient at deuterium in an axially symmetric C–D bond of length 1.095Å (2.0693 au). Because of the symmetry (Figure 4b), η is zero and we need only calculate the field gradient along the z-axis (principal axis system; z aligned with the C–D bond, $Z_n = +6$ au).

$$q_{zz}^{nuclear} = +\sum_n Z_n \frac{3z_n^2 - r_n^2}{r_n^5} = 1.3544 \text{ au} \tag{7}$$

Based on eqs 4 and 5, the other elements of the electric field gradient in the principal axis system are

$$q_{xx} = q_{yy} = \frac{-1}{2} q_{zz} \tag{8}$$

again making use of $\eta = 0$.

The conversion of electric field gradient values into frequency units allows for comparison with experimental data. Of course, the conversion factor requires an accurate value for the nuclear electric quadrupole moment:

$$C_Q[\text{Hz}] = e^2 q_{zz} Q/h \text{ [Hz]} = q_{zz}[\text{au}] \times \frac{e^2 Q}{4\pi\varepsilon_0 a_0^3 h} \tag{9}$$

where the field gradient, q_{zz}, is in atomic units, e is the electric charge in Coulombs, ε_0 is the vacuum permittivity, a_0 is the Bohr radius in meters, and h is Planck's constant. The value of the conversion factor, based on the currently accepted value of Q for the deuteron, is 672 kHz au^{-1}.

In frequency units, the quadrupole coupling constant (nuclear contribution only) for a deuteron in a C–D bond is +910 kHz. This is considerably larger than the experimentally measured value of the deuterium quadrupole coupling constant of +175 kHz for a typical C–D bond. The conclusion is that the electronic contribution is both negative and slightly smaller in magnitude than the nuclear contribution. At first glance, one might have expected the electronic contribution to have exactly the same magnitude as the nuclear term based on the absence of an overall electric charge. However, the r^{-3} averaging tends to emphasize the charges close to the deuteron (the carbon nucleus) and rapidly reduces the contribution from electron density distant from the deuteron site, *e.g.*, electron density in the other covalent bonds to carbon. For the HD molecule, a similar calculation shows that the nuclear contribution is 404 kHz ($r = 0.79$ Å); C_Q for the HD molecule is 225 kHz.[11] Again, the nuclear contribution is larger than the electronic contribution.

Returning to our initial concepts as expressed in Figures 1 and 2, we now see that

while the concepts are correct, they are not necessarily easily separable. While C_Q increases from LiD to DF, the origin of the increase is due to both increasing nuclear charge and shorter X–D bonds. It is true that the nuclear charge is only partially shielded by the core and valence electrons since C_Q is positive (based on a combination of experiments and calculations for HD through DF). The discontinuous drops in C_Q values between the data points for HD and LiD and between DF and AlD_4^- can be assigned to both increasing core and valence electron shielding and a longer X–D bond.

In summary, it is possible to qualitatively understand trends in C_Q and η for deuterium in a wide variety of sites based upon consideration of nuclear charge, bond distances, and local symmetry. In this sense, it is much easier to relate C_Q and η to molecular structure and bonding than to perform the corresponding analyses for chemical shielding tensors[12-15] or J-coupling tensors[16] where details of the molecular electronic wavefunction, especially excited molecular states, become so important.

Applications of Deuterium C_Q and η Values

C–D bonds

In principle, the value of C_Q for a deuteron in an X–D bond should be sensitive to the presence of excess electric charge on X. This principle was applied to a study of charge on carbon in the bridging methylene unit in cis-(μ-CD_2)(μ-CO)[FeCpCO]$_2$.[17] Earlier, a photoelectron study found an abnormally small C_{1s} binding energy; the low binding energy was interpreted by assigning a charge of $-0.5\ e$ on carbon relative to a model CH_2 unit.[18] A relative charge, Δq, of $-0.5\ e$ should reduce the value of C_Q; in the context of Figure 2, the shielding from the core and valence electrons is larger. The problem is deducing the proportionality constant between charge and ΔC_Q. One estimate for the value of $\Delta C_Q/\Delta q$ comes from a point charge model identical to the calculation leading to the nuclear contribution to C_Q for carbon. For a C–D bond length of 1.095 Å, the six protons of the carbon nucleus generate a field gradient at deuterium corresponding to $C_Q^{nuclear} = +910$ kHz. Since $C_Q^{nuclear}$ depends linearly upon charge, $\Delta C_Q/\Delta q = 152$ kHz e^{-1} indicating that deuterium NMR should be a very sensitive measure of charge on carbon in the bridging methylene unit. (Actually, a more realistic model for the spatial distribution of the excess charge is based upon a carbon $2p$ atomic orbital; the diffuse charge reduces $\Delta C_Q/\Delta q$ to 61.2 kHz e^{-1}.[17]) However, C_Q for the bridging methylene site in cis-(μ-CD_2)(μ-CO)[FeCpCO]$_2$ was not shifted to a lower value thus indicating a normal charge on carbon relative to the aliphatic model. Interestingly, C_Q values for other bridging methylene sites do indicate a small negative charge on carbon; perhaps there is a trans-effect from the bridging carbonyl that operates across the Fe—Fe bond.

The concept that C_Q can be affected by neighboring charges has been applied D–C–C–O systems. Here, X is oxygen and the oxygen nuclear charge creates a noticeable change in both C_Q and η. More importantly, the effect depends upon the position of the oxygen nucleus with respect to the much larger electric field gradient due to the directly bound carbon of the C–D bond. The result is a dependence upon the torsion angle in the D–C–C–O unit.[19] This result led to the first Karplus-type relationship[20] to be developed in solid-state NMR.[9,21] In the context of Figure 2,

additional charges are placed near the deuteron and each charge contributes to the electric field gradient at deuterium. (Note: because the electric field gradient is a tensor quantity, the effects of neighboring charges cannot be simply added.) The through-space effect from a neighboring oxygen atom in a D–C–C–O unit can be modeled as a function of the torsion angle of the unit with an equation that is similar to that used by Karplus to describe through-bond effects in ^{1}H NMR J-coupling.

C–D bond lengths have an influence upon C_Q. At this point, one should have sufficient familiarity with electric field gradients to make a qualitative prediction: shorter C–D bonds will have a larger nuclear contribution (which is positive) and therefore a larger value of C_Q (assuming a constant electronic contribution). Indeed, this is consistent with the experimental observation: sp^3 sites have C_Q values of 170–175 kHz,[7,9,17,21] aromatic sites are at 180–185 kHz, and sp sites have values greater than 200 kHz.[1,22,23] In the context of Figure 2, the variation in r for the different C–D sites will lead to different nuclear and electronic contributions to the electric field gradient at deuterium.

Hydrogen bonding

There have been a number of solid-state deuterium NMR studies of O–D$\cdots$O hydrogen bonding starting with the work of Chiba.[24] The structure of hydrogen bonds has a very large effect on the deuterium C_Q and η values. Hydrogen bonds range from nonexistent, for example, a gas phase water molecule, to exceedingly strong with an O$\cdots$O distance of only 2.4 Å; a weak hydrogen bond may have an O$\cdots$O distance up to 3 Å. Coupled with the O$\cdots$O distance is the O–D distance; the shorter, stronger hydrogen bonds have a longer O–D bond. In the limit of the very strong bonds with O$\cdots$O distances of only 2.4 Å, the deuterium is often at the midpoint of the bond, an O–D bond of 1.2 Å. This is much longer than the O–D bond length in an isolated water molecule of 0.957 Å.[25] Based on the previous discussion of the effect of X–D bond lengths on electric field gradients, one should expect a large variation in C_Q in hydrogen-bonding systems. Indeed, Chiba found in 1964 that short, strong hydrogen bond systems have smaller values of C_Q than do long, weak hydrogen bonds. In a summary of available data combined with a molecular orbital calculation of a model hydrogen bonding system, Brown and co-workers noted the consistency of the electric field gradient properties, especially the principal axis orientation, even in extremely non-linear hydrogen bonds.[26,27]. The conclusion one reaches is that the donor oxygen nuclear charges makes the largest contribution to the electric field gradient at deuterium. Hence, increasing the O–D bond length upon formation of a hydrogen bond will reduce the value of C_Q. In the context of Figure 2, an increase in r for the O–D bond sites will reduce the nuclear contribution to the electric field gradient at deuterium; additional effects are expected from neighboring charges such as the nucleus of the hydrogen bond acceptor oxygen atom, partly shielded by a negative electric charge often found on acceptor sites.

Based on the available data, the same principles noted for O–D$\cdots$O hydrogen bonds apply to N–D$\cdots$O and N–D$\cdots$N hydrogen bonds.[28,29] Given the importance of N–D$\cdots$O hydrogen bonds in biological systems, we anticipate interesting applications of deuterium NMR/NQR for structural studies. Probably the most difficult problem to overcome is that of overlapping resonances for a non-selectively

labeled biological species; otherwise, the interpretive methods are rather well developed.

Metal-deuterium bonds

For deuterium bound to metals, quadrupole coupling constants range from near zero to nearly that of the HD molecule. This wide range of C_Q values is, in the context of Figure 2, related to the metal nuclear charge, to the shielding by core and valence electrons, and to the wide range of M–D bond lengths. In addition, unusually symmetric environments can also reduce C_Q. In stoichiometric PdD, the deuterium sites have local octahedral symmetry, thus C_Q is near zero.[30] A few systems with terminal M–D bonds have been studied: LiD, 33 kHz;[31] Cp_2MoD_2, 52 kHz;[32] Cp_2WD_2, 54 kHz;[32] $DMn(CO)_5$, 68 kHz;[33] and $[Cp_2ZrD_2]_x$, 46.7 kHz;[3]. The relatively small values found in terminal M–D bonds are probably due both to a large electronic contribution and to the length of a M–D bond; the C_Q values are consistent with Salem's correlation between C_Q and the vibrational force constant.[22,34] Of all of these values, only that for LiD is known to be positive; C_Q is likely to be positive for all sites, but there are no experimental data.

Bridging metal hydride bonds have η values that depend upon $\angle$ M–D–M. The bridging metal hydrides. $[DCr_2(CO)_{10}]^-$ and $[DW_2(CO)_{10}]^-$, have structures that vary as a function of counterion; asymmetry parameters range from near zero to 0.31.[35] The values of C_Q and η have been analyzed with a simple point charge model with the assumption that the sign of C_Q is positive (we will discuss this assumption below). To date, the bridging metal hydride data and corresponding model represent the best starting point for analyzing deuterium NMR data of surface species on supported metal catalysts (work in progress in our lab).

Preliminary data and results from molecular orbital calculations of a model system show that C_Q and η vary in a predictable manner for the η^2-coordination of dihydrogen to a metal site. The model system indicates that C_Q and η slowly evolve until scission of the dihydrogen bond yields a cis-dihydride.[36] The limiting C_Q values are 225 kHz for the D_2 molecule and on the order of 50 to 80 kHz for the cis-dihydride. Kubas et al.[37] reported C_Q = 124 kHz for $W(CO)_3(P\text{-}i\text{-}Pr_3)_2(\eta^2\text{-}D_2)$, which is in good agreement with both the simple model of Figure 2 and the molecular orbital calculations.

Motional Effects

To this point, the discussion has been concerned with an electric field gradient tensor that has a constant orientation with respect to the laboratory axis system. In NMR spectroscopy, the magnet provides another interaction, the Zeeman interaction, and therefore, the question arises: Is the electric field gradient tensor stationary or in motion with respect to the orientation supplied by the magnetic field? Because of the well-defined values for C–D bonds (C_Q, η, orientation of the tensor), motional averaging effects are relatively easy to observe in the form of partially reduced values of C_Q, changes in the apparent value of η, or more rapid spin-lattice relaxation times.[19,38,42]

In organometallic complexes, the cyclopentadienyl ring is relatively free to rotate, even in the solid state.[43,44] Solid-state deuterium NMR is an ideal method for measuring Cp-ring rotation rates over a very wide range. In $(\mu\text{-}CO)_2[FeCp(CO)]_2$,

Cp-ring rotation rate constants of 2.4×10^{11} s^{-1} (300 K) down to 1.2×10^7 s^{-1} (110 K) were measured from a combination of line shape and T_1 data.[45] As an aside, the solution-state NMR spectroscopy of $(\mu\text{-CO})_2[FeCp(CO)]_2$, a textbook example of dynamical behavior, continues to be discussed and refined.[46]

Motional averaging and the resulting line shape changes have been used to follow the surface chemistry of absorbed molecules on supported metal catalysts. Slichter and coworkers determined the activation energy for the formation of ethylidyne on Pt/Al$_2$O$_3$ from ethylene and from acetylene + D$_2$.[47,48]

Sign of the Deuterium Quadrupole Coupling Constant

In Figure 2, the sign of C_Q is positive and all interpretative models to date are based on a positive value. However, there is some reason to suspect that the sign may be negative for some bridging metal hydride bonds; if so, the model must be improved, particularly for surface science studies. Experimetally, there are few methods for measuring the sign: gas-phase microwave spectroscopy[25] and NMR spectra showing both quadrupolar and dipolar interactions have been used.[49] Neither of these methods is generally useful in organometallic chemistry. However, at very high magnetic fields and very low temperatures, the Boltzmann distribution of spin state populations is such that the solid-state deuterium NMR line shape is skewed. The direction of skew, either to low frequency or high frequency, uniquely determines the sign of the deuterium quadrupole coupling constant. Shown in Figure 5 is the theoretical line shape for a M–D site with a positive quadrupole coupling constant at magnetic field of 18 Tesla and various temperatures. An 18 Tesla magnet is rather large, corresponding to a ^{1}H Larmor frequency of 766 MHz. The temperatures indicated in Figure 5 can be achieved with a ^{3}He/^{4}He dilution refrigerator. This experiment is somewhat easier to perform for nuclei with larger magnetogyric ratio or in ferromagnetic metals with large internal fields. Kuhns and Waugh[50] recently measured the sign of the ^{7}Li quadrupole coupling constant in LiNO$_3$ at 5.9 Tesla and the sign of C_Q for ^{165}Ho in ferromagnetic gadolinium was reported by Shaw *et al.*[51] In our lab, we are attempting to measure the sign of C_Q in bridging metal hydrides. The experiment is difficult mainly due to problems associated with the ^{3}He/^{4}He dilution refrigerator. Also, long deuterium spin-lattice relaxation times can render the experiment impossible in some systems. In spite of these difficulties, there is considerable importance associated with a correct model for C_Q and η so that metal hydrides can be studied and characterized on surfaces.

CONCLUSIONS

Deuterium quadrupole coupling constants and asymmetry parameters can be interpreted in terms of static structure and bonding and, in the case of motional average, can be used to measure the rate of motion. Relative to other NMR parameters, for example chemical shielding, electric field gradients are easier to interpret based upon a distribution of charges in the molecule. The recognition of the value of electric field gradients for studying chemical bonding is one of the many excellent contributions of Professor T. L. Brown.
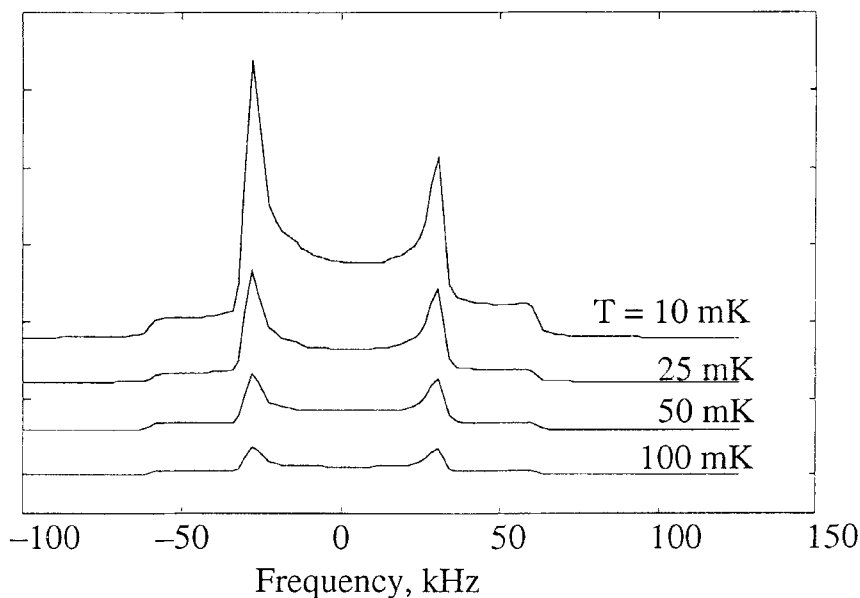
Figure 5 Simulated solid-state deuterium NMR line shapes at extremely high magnetic field and extremely low temperatures. Under these conditions, the sign of the deuterium quadrupole coupling constant can be obtained from the 'skew' of the line shape. The density matrix simulation is done for $C_Q = +80$ kHz, $\eta = 0$, $B_0 = 18$ Tesla, and a 1μs 90° pulse. The skew is reversed for $C_Q = -80$ kHz. The intensities of all traces are to scale and show the Curie-law increase in signal strength at low temperatures.

Acknowledgment

References

1. R. Bersohn *J. Chem. Phys.* **32**, 85 (1958).
2. P. Pyykkö, *Z. Naturforsch* **47a**, 189 (1992).
3. R.V. Reid Jr. and M.L. Vaida, *Phys. Rev. Lett.* **29**, 494 (1972).
4. R.V. Reid Jr. and M.L. Vaida, *Phys. Rev. Lett.* **34**, 1064 (1975).
5. C.P. Poole and H.A. Farach, *Theory of Magnetic Resonance* (Wiley-Interscience New York, 1987).
6. L.C. Snyder and H. Basch, *Molecular Wave Functions and Properties* (John Wiley & Sons New York, 1972).
7. L.C. Snyder. *J. Chem. Phys.* **68**, 291 (1978).
8. F.A. Cotton, *Chemical Applications of Group Theory*, 2nd ed. (John Wiley and Sons New York, 1971).

9. M.A. Jackisch, W.L. Jarrett, K. Guo, F.R. Fronczek, and L.G. Butler, *J. Amer. Chem. Soc.* **110**, 343 (1988).
10. As a rule of thumb for deuterium in small molecules, ab initio molecular orbital calculations, done with gaussian atomic orbitals at the level of double zeta or better, will yield reliable trends in electric field gradients as a function of structure, though the agreement with experiment may only be to within 20%.
11. N.F. Ramsey, *Molecular Beams* (Oxford University Press, p 238 New York, 1956).
12. W.H. Flygare, *Chem. Rev.* **74**, 653 (1974).
13. C.J. Jameson and J. Mason, 'The Chemical Shift' In *Multinuclear NMR*; Mason, J., Ed.; Plenum Press: New York, 1987.
14. A.J. Kim, M.I. Altbach, and L.G. Butler, *J. Amer. Chem. Soc.* **113**, 4831 (1991).
15. A.J. Kim and L.G. Butler, *Inorg. Chem.* **32**, 178 (1993).
16. G.H. Penner, W.P. Power, and R.E. Wasylishen, *Can. J. Chem.* **66**, 1821 (1988).
17. M.I. Altbach, Y. Hiyama, D.J. Gerson, and L.G. Butler, *J. Am. Chem. Soc.* **109**, 5529 (1987).
18. S.F. Xiang, H.W. Chen, C.J. Eyermann, W.L. Jolly, S.P. Smit, K.H. Theopold, R.G. Bergman, W.A. Herrmann, and R. Pettit, *Organometal.* **1**, 1200 (1982).
19. Y. Hiyama, S. Roy, K. Guo, L. G. Butler, and D. A. Torchia, *J. Am. Chem. Soc.* **109**, 2525 (1987).
20. M. Karplus, *J. Chem. Phys.* **30**, 11 (1959).
21. W.L. Jarrett, K. Guo, M.A. Jackisch, and L.G. Butler, *J. Magn. Reson.* **82**, 76 (1989).
22. L. Salem, *J. Chem. Phys.* **38**, 1227 (1963).
23. H. Huber, *J. Chem. Phys.* **83**, 4591 (1985).
24. T. Chiba. *J. Chem. Phys.* **41**, 1352 (1964).
25. P. Thaddeus, L.C. Krisher, and J.H.N. Loubser, *J. Chem. Phys.* **40**, 257 (1964).
26. L.G. Butler and T.L. Brown, *J. Am. Chem. Soc.* **103**, 6541 (1981).
27. T.L. Brown, L.G. Butler, D.Y. Curtin, Y. Hiyama, I.C. Paul, and R.B. Wilson, *J. Am. Chem. Soc.* **104**, 1172 (1982).
28. E.A. Keiter, Y. Hiyama, and T.L. Brown. *J. Mol. Struct.* **111**, 1 (1983).
29. Y. Hiyama, E.A. Keiter, and T.L. Brown, *J. Magn. Reson.* **67**, 202 (1986).
30. C.L. Wiley and F.Y. Fradin, *Phys. Rev. B* **17**, 3462 (1978).
31. L. Wharton, L.P. Gold, and W. Klemperer, *J. Chem. Phys.* **37**, 2149 (1962).
32. I.Y. Wei and B.M. Fung, *J. Chem. Phys.* **55**, 1486 (1971).
33. P.S. Ireland, L.W. Olson, and T.L. Brown, *J. Am. Chem. Soc.* **97**, 3548 (1975).
34. W.L. Jarrett, R.D. Farlee, and L.G. Butler, *Inorg. Chem.* **26**, 1381 (1987).
35. A.J. Kim, F.R. Fronczek, L.G. Butler, S. Chen, and E.A. Keiter, *J. Am. Chem. Soc.* **113**, 9090 (1991).
36. K. Guo, W.L. Jarrett, and L.G. Butler, *Inorg. Chem.* **26**, 3001 (1987).
37. G.J. Kubas, C.J. Unkefer, B.I. Swanson, and E. Fukushima, *J. Am. Chem. Soc.* **108**, 7000 (1986).
38. H.W. Spiess and H. Sillescu, *J. Magn. Res.* **42**, 381 (1981).
39. D.A. Torchia and A. Szabo, *J. Magn. Res.* **49**, 107 (1982).
40. D.A. Torchia, *Annu. Rev. Biophys. Bioeng.* **13**, 125 (1984).
41. L.W. Jelinski, *Annu. Rev. Mater. Sci.* **15**, 359 (1985).
42. M.A. Janusa, X. Wu, F.K. Cartledge, and L.G. Butler, *Envir. Scien. & Tech.* **27**, 1426 (1993).
43. E. Maverick and J.D. Dunitz, *Mol. Phys.* **62**, 451 (1987).
44. D. Braga, *Chem. Rev.* **92**, 633 (1992).
45. M.I. Altbach, Y. Hiyama, R.J. Wittebort, and L.G. Butler, *Inorg. Chem.* **29**, 741 (1990).
46. L.J. Farrugia and L. Mustoo, *Organometal.* **11**, 2941 (1992).
47. D.B. Zax, C.A. Klug. C.P. Slichter, and J.H. Sinfelt, *J. Phys. Chem.* **93**, 5009 (1989).
48. C.A. Klug, C.P. Slichter, and J.H. Sinfelt, *J. Phys. Chem.* **95**, 2119 (1991).
49. S.D. Swanson, S. Ganapathy, and R.G. Bryant, *J. Magn. Reson.* **73**, 239 (1987).
50. P.L. Kuhns and J.S. Waugh, *J. Chem. Phys.* **97**, 2166 (1992).
51. K.I. Shaw, I.S. MacKenzie, and M.A.H. McCausland, *J. Phys. F.: Met. Phys.* **13**, 1735 (1983).
52. A.C.H. Chan and E.R. Davidson, *J. Chem. Phys.* **49**, 727 (1968).
53. S.Z. Merchant and B.M. Fung, *J. Chem. Phys.* **50**, 2265 (1969).
54. P. Thaddeus, L.C. Krisher, and P. Cahill, *J. Chem. Phys.* **41**, 1542 (1964).
55. J.S. Muenter and W. Klemperer, *J. Chem. Phys.* **52**, 6033 (1970).
56. P. Pyykkö and B. Pedersen, *Chem. Phys. Lett.* **2**, 297 (1968).
57. B.M. Fung and I.Y. Wei, *J. Am. Chem. Soc.* **92**, 1497 (1970).
58. D.J. Genin, D.E. O'Reilly, T. Tsang, and E.M. Peterson, *J. Chem. Phys.* **48**, 4525 (1968).